IAES International Journal of Artificial Intelligence (IJ-AI)
Vol. 15, No. 2, April 2026, pp. 1623~1631
ISSN: 2252-8938, DOI: 10.11591/ijai.v15.i2.pp1623-1631

Analysis of tuberculosis detection using deep learning technique and explainable artificial intelligence

Shashikiran Srinivas[1], Kavita Avinash Patil[2], Kushalatha Monappa Rama[3], Sudha Venkateshlu[4], Jayanthi Muthuswamy[1], Srinivas Babu Narayanappa[1]
[1]Department of Electronics and Communication Engineering, New Horizon College of Engineering, Bengaluru, India
[2]Department of Electronics and Telecommunication Engineering, Ramaiah Institute of Technology, Bengaluru, India
[3]Department of Electronics and Communication Engineering, Nitte Meenakshi Institute of Technology, NITTE (Deemed to be University), Bengaluru, India
[4]Department of Computer Science and Engineering, Amity University, Bengaluru, India

Article Info

Article history:

Received Sep 26, 2024
Revised Jan 30, 2026
Accepted Feb 6, 2026

Keywords:

Accuracy
Convolutional neural network
DenseNet-121
Grad-CAM
Transfer learning

ABSTRACT

Tuberculosis (TB) affects the health of many individuals and is still a prime worldwide health concern despite having so many advanced treatments, as it still lacks technical advancement in its treatment and diagnosis. Accuracy in identification and early detection is essential to reduce the spread and improve treatment outcomes. Traditional methods of diagnosis, such as sputum microscopy and culture, are labor-dependent and subject to human mistakes as it is done by lab technicians. Recent improvements in deep learning have demonstrated significant potential for enhancing and automating diagnostic accuracy. Our research proposes a deep learning-based technique that detects TB from chest X-rays after image processing techniques like augmentation. After training on big data, our model pulls off an astonishing accuracy of 97.42% and a loss of 7.17%, outperforming traditional methods. The model uses convolutional neural network (CNN) as a base and transfer learning method, like DenseNet-121, and explainable artificial intelligence (XAI) technique, like Grad-CAM, to recognize TB-related patterns effectively and with low false positives. This approach has the ability to revolutionize the diagnosis of TB and offer more dependable, scalable, and timely solutions to healthcare systems worldwide.

Corresponding Author:

Kavita Avinash Patil
Department of Electronics and Telecommunication Engineering, Ramaiah Institute of Technology, Bengaluru, India.
Email: kavitamalagatti@gmail.com

1. INTRODUCTION

Mycobacterium tuberculosis (Mtb), the bacteria that causes tuberculosis (TB) [1], continues to be a major public health concern, with many new cases and deaths each year. Despite significant advancements in public health and medicine, TB remains a prime cause of death and morbidity, particularly in underdeveloped countries where access to healthcare units is limited. Sputum [2] smear microscopy [3] and chest X-rays [4] are two essential traditional diagnostic techniques [5] for TB. Even with these developments, problems including limited sensitivity, high false-negative rates, and inconsistent diagnostic accuracy might occasionally limit these techniques. An innovative solution to these issues is offered by deep learning [6], a potent branch of artificial intelligence [7]. By increasing the precision and automation of complicated pattern detection in images [8], deep learning [9] has significantly changed the area of medical imaging [10]. This is especially true when using convolutional neural networks (CNNs) [11]. These developments are particularly

aids in the identification of TB [12], since CNN's are groomed to identify subtle abnormalities that traditional approaches [13] are unable to identify. TB is usually curable and preventable.

It is possible to successfully modify pretrained structures [14] for radiological interpretation pertinent to a particular area. DenseNet-121 [15] is especially useful for TB detection [16] due to its densely connected feature propagation, which improves gradient stability and permits the recovery of fine-scale parenchymal patterns [17] linked to TB lesions. The model's [18] capacity to generalize is enhanced by combining DenseNet-121 with particular imbalance-handling processes, such as minority-class frequencies as low as 10–20%, employing synthetic minority oversampling technique (SMOTE) [19] and associated hybrid resampling techniques. DenseNet-121, a deep CNN [20], is widely used for image classification applications, such as TB identification from chest X-ray pictures. To reduce overfitting and enhance feature propagation, densely linked layers are employed. In order to effectively identify patterns associated with TB, DenseNet-121 is used on a labeled dataset. The areas of the X-ray [21] that are most crucial to the model's completion are then displayed [22] using gradient-weighted class activation mapping or Grad-CAM [23]. Grad-CAM draws attention to these areas to make DenseNet-121's forecasts easier to understand. This machine facilitates precise diagnosis [24], boosts physician trust in artificial intelligence models, and enables them to understand the logic underlying classification.

Furthermore, the process of detecting and diagnosing TB [25] will be accelerated and made simpler by using deep learning and artificial intelligence. The majority of earlier research on the diagnosis and detection of TB [26] was concentrated on image processing methods, using MATLAB and simple CNN networks as a detection model. This research article is divided into five sections: section 1 introduces the disease TB and the use of deep learning to diagnose it; section 2 provides an overview of earlier research that is relevant to this study; section 3 illustrates the suggested method and how it is implemented; section 4 shows the findings; and finally, section 5 provides the summary, which is followed by a list of references. The results of this work are as follows: i) TB is detected from chest X-ray images using CNN, ii) the transfer learning technique known as DenseNet-121 is used, which improves classification accuracy using specified weights, iii) To better display and comprehend the output, the explainable artificial intelligence (XAI) [27] approach known as Grad-CAM is employed.

2. RELATED WORK

Panicker *et al.* [2] explains an automatic method for identifying TB bacilli from pictures of microscopic sputum images. According to data from the World Health Organization (WHO), TB is the tenth most prevalent cause of mortality globally. Although there are several ways to diagnose TB, the conventional microscopic analysis of sputum smears is considered the standard technique. The diagnosis procedure is long and erroneous, even when performed by professionals. The proposed algorithm for TB identification achieves 86.76%-F1-score, 78.4%-precision, and 97.13%-recall based on experimental data. This automatic method tells whether or not the sputum smear pictures indicate TB infection.

Kabir *et al.* [7] clarifies that chest radiography is a crucial diagnostic technique for diseases like TB, pneumonia, and COVID-19 because it gives a realistic representation of the architecture of the chest. However, effectively identifying these illnesses from radiographs is a challenging task that requires medical imaging technology. Conventional deep learning models offer a practical automated solution for this issue. However, because these models are so sophisticated, their practical deployment in medical applications often encounters significant obstacles. By using knowledge distillation techniques (KDT) to lessen the complexity of CNN, this work addresses and resolves this puzzle.

Hassan *et al.* [19] adds that deep learning techniques for knee osteoarthritis (KOA) detection have been more prominent in recent years. Also, how to create a deep learning model for KOA detection using knee X-ray images and the Kellgren–Lawrence (KL) grading system. The knee osteoarthritis classification network (KOC_Net), a novel CNN-based model, is proposed in this paper. Two publicly accessible benchmark datasets comprising X-ray images of KOA based on the KL grading system are used to assess the KOC_Net model. Additionally, we used SMOTE Tomek to solve the issue of minority classes and contrast-limited adaptive histogram equalization (CLAHE) techniques. With an area under the curve (AUC)-96.71%, accuracy-96.51%, recall-91.95%, precision- 90.25%, and F1-score of 96.70%, the suggested KOC_Net was able to categorize KOA into five different groups.

Rony *et al.* [27] briefs that, in order to improve the precision and dependability of autism spectrum disorder (ASD) diagnosis, this study used sophisticated machine-learning algorithms. We used a standard dataset with 20 variables and 1,054 patient samples. At 99%, the suggested diabetes mellitus and logistic regression with Shapley additive explanations (DMLRS) model outperformed cutting-edge techniques. To improve interpretability, Shapley additive explanations (SHAP) were used to integrate XAI. Each technique

was refined, and k-fold cross-validation was used to confirm performance. Additionally, a real-time web application that combines the Django framework for ASD detection with the DMLRS model was created.

Shahshikiran *et al.* [28] briefs that, *Mycobacterium* causes TB, a deadly illness. Managing TB infections requires early detection and identification of the disease. As this study shows, recent technical advancements employ a machine learning (ML)-based support vector machine (SVM) and CNN, which is modified to more precisely detect particular diseases. Throughout construction, the enhanced feature extraction and classification accuracy of the updated CNN are preserved. The TBX11K publicly available dataset, which includes 11,000 images—4,600 of which are chest X-ray images—is used to achieve good performance, and the proposed model is validated. The accuracy of TB identification using SVM is 93.14%, while the accuracy using modified CNN is 96.72%.

3. METHOD

Several essential procedures are typically involved in deep learning-based project-related work for TB diagnosis. The block diagram for the approach employed is shown in Figure 1. It is made up of several blocks that use the chest X-ray dataset's images as input, apply a transfer learning model, and then classify the query image using the information learned from the model's training.

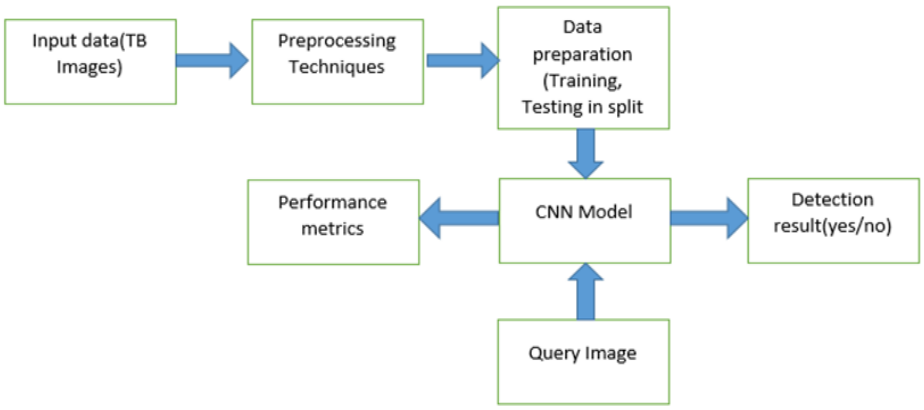

Figure 1. Block diagram for the proposed technique

3.1. Dataset availability and preparation

Loading metadata and images: initially, X-ray images and the associated metadata were all over the place. The collection contains two types of chest X-ray images: normal and TB-infected. We were able to distinguish between healthy people and TB patients since the dataset was pre-labeled. Figure 2 shows the sample of TB images of dataset, where uninfected are in Figure 2(a) and infected are in the Figure 2(b). Data segmentation for training, validation, and testing: the following image distribution is provided to ensure consistent model performance: the national institute of allergy and infectious diseases (NIAID) TB portal program dataset was utilized in this study for the classification stage of the experiment. The "tuberculosis" Kaggle project's "chest X-ray pictures dataset", which contained 700 TB images and 3,500 normal images, is where this dataset originated. All 700 TB of the control chest X-ray images were utilized. With total images being 4,200 the split ratio =0.2. Therefore, training images =(2,800 normal+560 TB images) and test images =(700 normal+140 TB images).

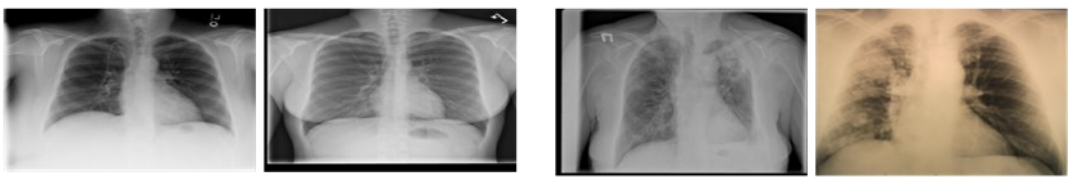

(a) (b)

Figure 2. Sample images figure for (a) TB images-uninfected and (b)TB images-infected

3.2. Data preprocessing

3.2.1. Generating train data

The images were scaled, normalized, and improved using rotation, magnification, and flipping algorithms to improve generalization in order to fit into the network design. A train generator was built to swiftly import the training data and perform on-the-spot preprocessing.

- Normalize the mean and standard deviation (SD) of every data set.
- Shuffle the input after each epoch.
- Verify that the image is 320 by 320 pixels. To balance computational speed and diagnostic accuracy, all chest X-ray pictures were modified to 320×320 pixels.
- Implement some modifications (rotation, zoom, width shift, and height shift) based on position deviation, which may change slightly when radiologists X-ray patients.
- In the next step, it happens inside the generator tool-grayscale X-ray pictures gain depth when their data fills each of the 3 color paths. Since the ready-made model only works with 3-layer inputs, this shift makes it run.

3.2.2. Generating test and validation data

The same data were created for the test and validation datasets without any augmentations in order to preserve the integrity of the evaluation process. To verify that the preprocessing was done correctly, a normalized picture sample from the training generator was displayed. The images had pixel values between 0 and 1, and they were resized to match the model's required input shape.

- We normalize incoming test and validation data using the statistics estimated from the training set.
- To save computational time, we computed the sample mean (SM) and sample SD using a random sample from the dataset (ideally, the full training set should be used for calculating the SM and SD). Figure 3 illustrates the uneven data distribution before image augmentation. Additionally, Figure 4 displays a balanced data distribution following image augmentation. The sample weighting fix for the loss function. Creating+ve (positive) and -ve (negative) contributors.

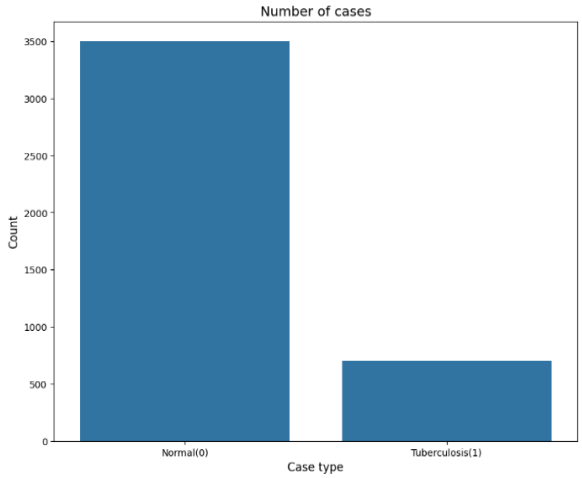

Figure 3. Imbalance data (uneven data)

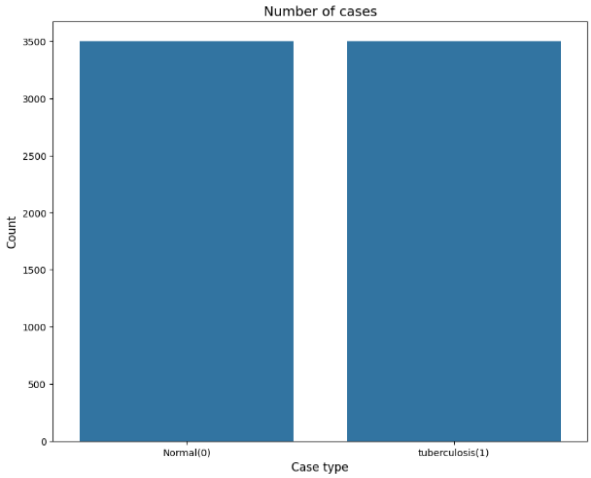

Figure 4. Balance data (even data)

This study's weighted loss formulation balances positive and negative contributions, as indicated in (1) and (2). The frequency of negative and positive samples determines the positive-class weight (Wp) and negative-class weight (Wn), respectively. These weights were then added to the weighted cross-entropy loss described in (3). The following calculation provides the final weight loss to be used in the DenseNet-121 architecture as in (3).

$$W_{pos} \times F_P = W_{neg} \times F_n \quad (1)$$

$$W_{pos} = F_n \& W_{neg} = F_P \quad (2)$$

$$L_{ce}^{w} = -(W_P.y.\log(f(x)) + W_n(1-y)\log(1-f(x) \quad (3)$$

To address the question concerning empirical validation, we ran comparison tests on model performance without and with weighted loss functions. The new data clearly explain that the weighting technique improves sensitivity, F1-score, and Matthews correlation coefficient (MCC) for the TB-positive class while also lowering the false-negative rate, which is an important indicator of reduced majority-class bias. The transformer-dependent denoising methodology [27] takes a methodical approach to preserving diagnostic detail while reducing acquisition-related noise, potentially increasing the quality of DenseNet-121's chest X-ray inputs.

3.3. Transfer learning integration with deep learning (DenseNet-121+CNN)

DenseNet-121, a powerful CNN pre-trained on the ImageNet dataset, for transfer learning. By leveraging pre-learned features, the model gains the potential to enhance accuracy and faster convergence with a smaller dataset. The number "121" indicates that the transfer learning model in issue has 121 layers. The mathematical breakdown of DenseNet-121 is as follows: combined function: each layer applies a composite function H_l that includes as in (4).

$$H_l(x) = W_l([x_0, x_1..x_{l-1}]) \quad (4)$$

Where $H_l(x)$–l_{th} layer output, W_l–l_{th} layer weights, $[x_0, x_1..x_{l-1}]$–feature maps.

Transition layer: DenseNet uses a transition layer that performs a convolution and then pooling to regulate the size of feature maps. The following is the mathematical expression for the transition layer as (5).

$$H_t(x) = Pooling(BN(W_{conv}(x))) \quad (5)$$

Where $H_t(x)$–l_{th} layer output, W_{conv}–l_{th} layer weights, BN–batch normalization.

A single layer's output size depends on how many feature maps it creates. This amount climbs with each step because of a setting called the growth rate, labeled *k*. Each new layer adds exactly *k* more mappings than the one before. The pattern continues consistently through the network and is given as (6).

$$F_l = F_0 + l.k \quad (6)$$

Where: F_l–l^{th} layer output feature maps, F_0–1st feature maps.

Dense block (DB): DenseNet-121 consists of four DBs, each with a distinct number of layers. Transition layer follows every block, with the exception of the last one. The exact layer counts of DenseNet-121 are as follows: six layers make up DB 1, twelve in DB 2, twenty-four in DB 3, and sixteen in DB 4. The final DenseNet-121 formula is shown as (7), with f–DB, t–transition layer, and P–output following global average pooling.

$$P = DenseNet121(X) = f_4(t_4\left(f_3\left(t_3\left(f_2\left(t_1(f_1(X))\right)\right)\right)\right) \quad (7)$$

3.4. Explainable artificial intelligence (Grad-CAM)

The model pays attention to a TB image that comes clear through Grad-CAM. One layer at a time gets picked by the system to map out what matters for sorting images into types. Medical pictures gain clarity since these maps highlight spots likely affected. Infection zones stand out where color intensifies on the overlay. Our setup uses Grad-CAM to sketch where attention should go, shaped by shifts across layers. Emerging XAI methods [29] in medical fields. Their employment of complementary explainability mechanisms illustrates the potential benefit of combining advanced visualization techniques like Grad-CAM++, Score-CAM, or attention-based interpretability to provide more granular and clinically useful explanations in TB categorization.

4. RESULTS AND DISCUSSION

Classification report:

- Precision: the true positive (TP) classification ratio to the total number of TP+false positives (FP) is known as precision.

$$Precision = \frac{TP}{TP+FP} \quad (8)$$

– Recall: recall is essential to determine capacity of the deep learning model to detect positive samples. Compared to sensitivity, recall is concerned only with how positives are classified.

$$Recall = \frac{TP}{TP+FN} \quad (9)$$

– F1-score: another common name for F1-score–F measure. To achieve the balance in between precision and recall, we need a larger number of true negatives (TN) and TP in the model, and the F1-score allows us to choose the ideal confidence level.

$$F1-score = \frac{2(Precision*Recall)}{Precision+Recall} \quad (10)$$

– Accuracy: the sum of TN and TP classification ratio to the total instants.

$$Accuracy = \frac{TP+TN}{TP+TN+FP+FN} \quad (11)$$

Within the confusion matrix (CM) are four values: TP, TN, FP, and false negatives (FN). With counts standing at 463 for TP, alongside 429 for TN, false outcomes appear less often; specifically, FP reaches 12, while FN settles at 6. Accuracy measures 97.42 percent, since each precision nears 97.4% and recall climbs to 98.7%, and hence the F1-score aligns closely at 98.0%. At the seventeenth training cycle, Figure 5 displays CNN achieving exactly 97.42% accuracy. Meanwhile, loss drops notably by that stage–Figure 6 records it as lows as 0.0717 when epoch count hits twenty.

Grad-CAM heatmaps determine which lung regions have the greatest impact on a model's diagnosis for TB detection. The model's focus on abnormal areas, such as lesions or sick tissue, can be clearly seen by superimposing the heatmap on chest X-rays. Figure 7 illustrates the Grad-CAM overlay those results from superimposing the Grad-CAM heatmap over the TB sample.

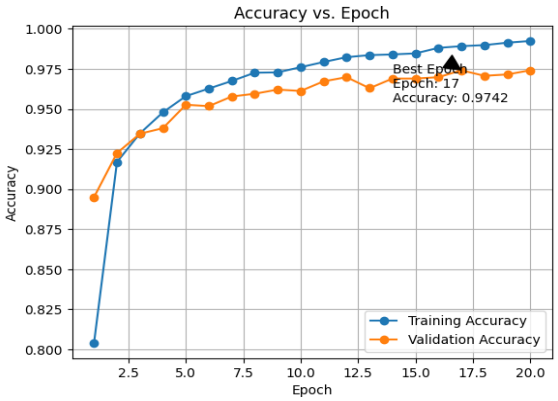

Figure 5. Accuracy vs. epoch plot

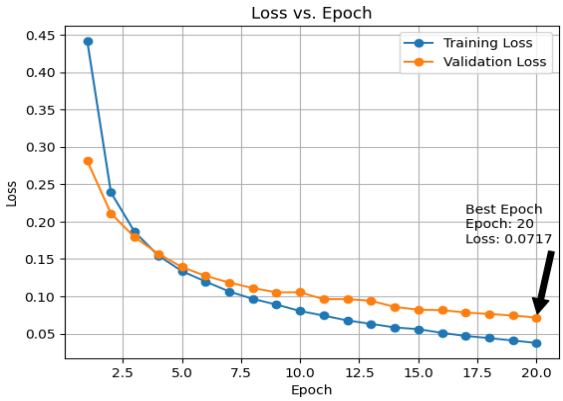

Figure 6. Loss vs. epoch plot

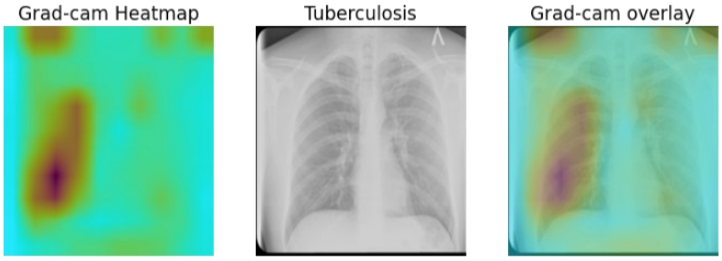

Figure 7. Grad-CAM heat map with result overlay

5. CONCLUSION

A trained DenseNet-121 forms the base of this study's approach to identifying TB within chest X-rays. Instead of building from scratch, prior knowledge guides adaptation through transfer learning, shaping detection capability. Attention shifts toward key regions emerge via Grad-CAM, revealing where in each image decisions originate. Performance stays balanced between positive and negative cases, even when sample numbers differ. Adjustments such as weighted penalties and expanded datasets help stabilize outcomes. Precision holds high, recall follows closely, showing consistent reliability. Error rate settles at 7.17%, while correct classifications reach 97.42%. Visual explanations grow clearer once heatmaps overlay the original scans. Understanding improves–not just for machines, but for those who interpret results. Trust builds slowly when reasoning becomes visible. In clinical settings, seeing why matters as much as what is seen. Following training, evaluation occurred through multiple metrics. Overall success emerged when Grad-CAM paired with DenseNet-121, pointing toward usefulness in detecting TB automatically within medical imaging contexts.

FUNDING INFORMATION

Authors state no funding involved.

AUTHOR CONTRIBUTIONS STATEMENT

This journal uses the Contributor Roles Taxonomy (CRediT) to recognize individual author contributions, reduce authorship disputes, and facilitate collaboration.

Name of Author	C	M	So	Va	Fo	I	R	D	O	E	Vi	Su	P	Fu
Shashikiran Srinivas	✓	✓	✓	✓	✓	✓		✓	✓	✓		✓	✓	
Kavita Avinash Patil		✓	✓	✓	✓	✓		✓	✓	✓	✓	✓		
Kushalatha Monappa Rama			✓		✓	✓	✓	✓		✓	✓			
Sudha Venkateshlu			✓		✓	✓	✓			✓				
Jayanthi Muthuswamy	✓	✓	✓	✓	✓	✓		✓	✓	✓		✓	✓	
Srinivas Babu Narayanappa	✓	✓	✓	✓	✓	✓		✓	✓	✓	✓	✓	✓	

C : **C**onceptualization
M : **M**ethodology
So : **So**ftware
Va : **Va**lidation
Fo : **Fo**rmal analysis
I : **I**nvestigation
R : **R**esources
D : **D**ata Curation
O : Writing - **O**riginal Draft
E : Writing - Review & **E**diting
Vi : **Vi**sualization
Su : **Su**pervision
P : **P**roject administration
Fu : **Fu**nding acquisition

CONFLICT OF INTEREST STATEMENT

Authors state no conflict of interest.

INFORMED CONSENT

We have obtained informed consent from all individuals included in this study.

ETHICAL APPROVAL

The research pertaining to human use has been authorized by the institutional review board or comparable committee of the authors and has complied with all applicable national rules and institutional policies in accordance with the tenets of the Helsinki Declaration.

DATA AVAILABILITY

The authors confirm that the data supporting the findings of this study are available within the article.

REFERENCES

[1] World Health Organization, *Global tuberculosis report 2023*. Geneva, Switzerland: World Health Organization, 2023.

[2] R. O. Panicker, K. S. Kalmady, J. Rajan, and M. K. Sabu, "Automatic detection of tuberculosis bacilli from microscopic sputum smear images using deep learning methods," *Biocybernetics and Biomedical Engineering*, vol. 38, no. 3, pp. 691–699, 2018, doi: 10.1016/j.bbe.2018.05.007.

[3] T. F. M. Carvalho *et al.*, "A systematic review and repeatability study on the use of deep learning for classifying and detecting tuberculosis bacilli in microscopic images," *Progress in Biophysics and Molecular Biology*, vol. 180–181, pp. 1–18, 2023, doi: 10.1016/j.pbiomolbio.2023.03.002.

[4] V. Sharma, Nillmani, S. K. Gupta, and K. K. Shukla, "Deep learning models for tuberculosis detection and infected region visualization in chest X-ray images," *Intelligent Medicine*, vol. 4, no. 2, pp. 104–113, May 2024, doi: 10.1016/j.imed.2023.06.001.

[5] G. Tavaziva *et al.*, "Diagnostic accuracy of a commercially available, deep learning-based chest X-ray interpretation software for detecting culture-confirmed pulmonary tuberculosis," *International Journal of Infectious Diseases*, vol. 122, pp. 15–20, 2022, doi: 10.1016/j.ijid.2022.05.037.

[6] S. Hansun, A. Argha, S.-T. Liaw, B. G. Celler, and G. B. Marks, "Machine and deep learning for tuberculosis detection on chest X-rays: systematic literature review," *Journal of Medical Internet Research*, vol. 25, Jul. 2023, doi: 10.2196/43154.

[7] M. M. Kabir, M. F. Mridha, A. Rahman, M. A. Hamid, and M. M. Monowar, "Detection of COVID-19, pneumonia, and tuberculosis from radiographs using AI-driven knowledge distillation," *Heliyon*, vol. 10, no. 5, 2024, doi: 10.1016/j.heliyon.2024.e26801.

[8] A. Aljuaid and M. Anwar, "Survey of supervised learning for medical image processing," *SN Computer Science*, vol. 3, no. 4, May 2022, doi: 10.1007/s42979-022-01166-1.

[9] M. Nijiati *et al.*, "Deep learning and radiomics of longitudinal CT scans for early prediction of tuberculosis treatment outcomes," *European Journal of Radiology*, vol. 169, 2023, doi: 10.1016/j.ejrad.2023.111180.

[10] S. Vats *et al.*, "Incremental learning-based cascaded model for detection and localization of tuberculosis from chest X-ray images," *Expert Systems with Applications*, vol. 238, 2024, doi: 10.1016/j.eswa.2023.122129.

[11] R. Duwairi and A. Melhem, "A deep learning-based framework for automatic detection of drug resistance in tuberculosis patients," *Egyptian Informatics Journal*, vol. 24, no. 1, pp. 139–148, 2023, doi: 10.1016/j.eij.2023.01.002.

[12] N. Shome, R. Kashyap, and R. H. Laskar, "Detection of tuberculosis using customized MobileNet and transfer learning from chest X-ray image," *Image and Vision Computing*, vol. 147, 2024, doi: 10.1016/j.imavis.2024.105063.

[13] M. Alshutbi, Z. Li, M. Alrifaey, M. Ahmadipour, and M. M. Othman, "A hybrid classifier based on support vector machine and Jaya algorithm for breast cancer classification," *Neural Computing and Applications*, vol. 34, no. 19, pp. 16669–16681, 2022, doi: 10.1007/s00521-022-07290-6.

[14] A. Iqbal, M. Usman, and Z. Ahmed, "An efficient deep learning-based framework for tuberculosis detection using chest X-ray images," *Tuberculosis*, vol. 136, 2022, doi: 10.1016/j.tube.2022.102234.

[15] E. T. Hastuti, A. Bustamam, P. Anki, R. Amalia, and A. Salma, "Performance of true transfer learning using CNN DenseNet-121 for COVID-19 detection from chest X-ray images," in *InHeNce 2021 - 2021 IEEE International Conference on Health, Instrumentation and Measurement, and Natural Sciences*, 2021, pp. 1–5. doi: 10.1109/InHeNce52833.2021.9537261.

[16] P. K. Das, S. Sreevatsav, and A. Abraham, "An efficient deep learning network with orthogonal softmax layer for automatic detection of tuberculosis," *Engineering Applications of Artificial Intelligence*, vol. 133, 2024, doi: 10.1016/j.engappai.2024.108116.

[17] S. H. Abdullah, W. M. S. Abedi, and R. M. Hadi, "Enhanced feature selection algorithm for pneumonia detection," *Periodicals of Engineering and Natural Sciences*, vol. 10, no. 6, pp. 168–180, 2022, doi: 10.21533/pen.v10i6.3397.

[18] S. Chattoraj, B. Reddy, M. Tadepalli, and P. Putha, "Comparing deep learning models for tuberculosis detection: a retrospective study of digital vs. analog chest radiographs," *Indian Journal of Tuberculosis*, vol. 72, pp. S43–S46, May 2025, doi: 10.1016/j.ijtb.2024.05.008.

[19] S. N. Hassan, M. Khalil, H. Salahuddin, R. A. Naqvi, D. Jeong, and S. W. Lee, "KOC_Net: impact of the synthetic minority over-sampling technique with deep learning models for classification of knee osteoarthritis using Kellgren–Lawrence X-ray grade," *Mathematics*, vol. 12, no. 22, 2024, doi: 10.3390/math12223534.

[20] B. N. Srinivas, S. Shashikiran, M. Jayanthi, N. Rajani, K. M. Palaniswamy, and M. R. Kushalatha, "Tuberculosis classification using SVM and modified CNN," *Iranian Journal of Electrical and Electronic Engineering*, vol. 20, no. 4, pp. 126–133, 2024, doi: 10.22068/IJEEE.20.4.3463.

[21] M. Nijiati *et al.*, "Deep learning on longitudinal CT scans: automated prediction of treatment outcomes in hospitalized tuberculosis patients," *iScience*, vol. 26, no. 11, 2023, doi: 10.1016/j.isci.2023.108326.

[22] T. Rahman *et al.*, "Reliable tuberculosis detection using chest X-ray with deep learning, segmentation and visualization," *IEEE Access*, vol. 8, pp. 191586–191601, 2020, doi: 10.1109/ACCESS.2020.3031384.

[23] R. Lokare, J. Wadmare, S. R. Patil, G. Wadmare, and D. Patil, "Transparent precision: explainable artificial intelligence empowered breast cancer recommendations for personalized treatment," *IAES International Journal of Artificial Intelligence*, vol. 13, no. 3, pp. 2694–2702, 2024, doi: 10.11591/ijai.v13.i3.pp2694-2702.

[24] R. Geethamani and A. Ranichitra, "Enhancing tuberculosis detection: leveraging RF-HOG model for automated diagnosis from chest X-ray images," *Procedia Computer Science*, vol. 230, pp. 21–32, 2023, doi: 10.1016/j.procs.2023.12.057.

[25] G. Tamura, G. Llano, A. Aristizábal, J. Valencia, L. Sua, and L. Fernandez, "Machine-learning methods for detecting tuberculosis in Ziehl-Neelsen stained slides: a systematic literature review," *Intelligent Systems with Applications*, vol. 22, 2024, doi: 10.1016/j.iswa.2024.200365.

[26] C. Ying *et al.*, "T-SPOT with CT image analysis based on deep learning for early differential diagnosis of nontuberculous mycobacteria pulmonary disease and pulmonary tuberculosis," *International Journal of Infectious Diseases*, vol. 125, pp. 42–50, 2022, doi: 10.1016/j.ijid.2022.09.031.

[27] M. A. T. Rony *et al.*, "Innovative approach to detecting autism spectrum disorder using explainable features and smart web application," *Mathematics*, vol. 12, no. 22, 2024, doi: 10.3390/math12223515.

[28] S. Shahshikiran, N. Srinivas Babu, S. Pramanik, and Sathwik, "A modified deep learning architecture for detecting MalariaInfected cells," in *2024 International Conference on Knowledge Engineering and Communication Systems, ICKECS 2024*, 2024. doi: 10.1109/ICKECS61492.2024.10617005.

[29] R. A. Naqvi, A. Haider, H. S. Kim, D. Jeong, and S. W. Lee, "Transformative noise reduction: leveraging a transformer-based deep network for medical image denoising," *Mathematics*, vol. 12, no. 15, 2024, doi: 10.3390/math12152313.

BIOGRAPHIES OF AUTHORS

Shashikiran Srinivas in affiliation with Visvesveraya Technological University, Belagavi-590018. He is a research scholar at the Department of Electronics and Communication Engineering, R.R. Institute of Technology, Bangalore, India, and a faculty at the Department of Electronics and Communication Engineering, New Horizon College of Engineering, Bangalore, India. He was awarded the B.E. in ECE. Visvesveraya Technological University-PG Center Bangalore awarded him M.Tech. in DECS. At Visvesveraya Technological University in Belagavi, he is working toward a Ph.D. His areas of interests are medical image analysis, artificial intelligence, and image/signal processing. Based on his creative ideas, he has published 6 patents as first inventor, 2 UGC care journals, 6 IEEE Scopus indexed conference papers, 2 Q3 journal, 1 SCI paper and received the NMIT Conference 2024's "Best paper award" for one of his articles. He can be contacted at email: shashikiran067@gmail.com.

Kavita Avinash Patil received her B.E. in Telecommunication Engineering from the K. L. E. College of Engineering Belgaum in 2010 and the M.Tech. in VLSI Design and Embedded system from K. L. E. College of Engineering Belgaum in 2012. She received her Ph.D. degree in Electrical and Electronics Engineering from Visvesvaraya Technological University in June 2023. Presently she is working as an assistant professor in the Department of Electronics and Telecommunication Engineering, at Ramaiah Institute of Technology, Bangalore. Her research interest includes biomedical engineering, machine learning, data science, and artificial intelligence. Total 13 years of teaching experience. She can be contacted at email: kavitamalagatti@gmail.com.

Kushalatha Monappa Rama received her B.E. in Electronics and Communication Engineering from PA College of Engineering, Mangalore in 2005, affiliated to VTU, Belgaum and her M.Tech. in Digital Communication from BMS College of Engineering, Bengaluru, affiliated to VTU, Belgaum in 2014. She completed her Ph.D. from VTU. Presently, she is working as assistant professor in Department of Electronics and Communication Engineering in Nitte Meenakshi Institute of Technology (Deemed to be University), Bengaluru. Her research areas include signal processing, remote sensing, machine learning, and data science. She has total of 16 years of teaching experience. She can be contacted at email: kushalatha.mr@nmit.ac.in.

Sudha Venkateshlu is a research scholar at the Department of Electronics and Communication Engineering, SJB Institute of Technology, Bengaluru, India and faculty at the Department of Computer Science and Engineering, Amity University, Bengaluru. She received the B.E. degree RV College of Engineering. She received the M.Tech. degree in RV College of Engineering from Visvesveraya Technological University–PG Center Bangalore. She is pursuing a Ph.D. at Visvesveraya Technological University, Belagavi. Her research areas are artificial intelligence, machine learning, and medical image analysis. She has filed 3 patents on her innovative ideas. She has published 2 IEEE Scopus indexed conference papers, 2 UGC care journals, and 1 scopus indexed journal. She can be contacted at email: sudhaviju1@gmail.com.

Jayanthi Muthuswamy received her Ph.D. degree in Electrical and Electronics Engineering, Visvesvaraya Technological University, Belagavi, India, 2019. She is currently working as associate professor in Electronics and Communication Engineering, New Horizon College of Engineering, Bangalore. She has authored or coauthored more than 32 refereed journal and conference papers. Her research interests include digital signal processing, biomedical signal and image processing, IoT, and machine learning. She can be contacted at email: jayanthisathish1012@gmail.com.

Srinivas Babu Narayanappa is an assistant professor at the Department of Electronics and Communication Engineering, New Horizon College of Engineering affiliated with Visveswaraya Technological University, Belagavi 590018 India. He holds an M.Tech., degree in Digital Communication and Networking with a research specialization in medical image analysis. His research areas are image/signal processing, biometrics, medical image analysis, and pattern recognition. He has filed some design patents on his innovative ideas. He can be contacted at email: sribabu6887@gmail.com.